

# Correlated Interference from Uncorrelated Users in Bounded Ad Hoc Networks with Blockage

Konstantinos Koufos, Carl P. Dettmann and Justin P. Coon

**Abstract**—In this letter, we study the joint impact of user density, blockage density and deployment area on the temporal correlation of interference for static users and users with uncorrelated mobility. Even if the user locations are uncorrelated over time, the interference level can still be correlated when the deployment area is bounded and/or there is blockage. We also show that at a high blockage density, the temporal correlation coefficients increase with the user-to-blockage density ratio.

**Index Terms**—Blockage, Correlation, Interference, Mobility.

## I. INTRODUCTION

THE correlation of interference over sequential periods of time is an important quantity to study because it affects the correlation of receiver outage, the end-to-end delay, the handoff rate etc. [1], [2]. It arises due to correlations in the propagation channel and the Medium Access Control (MAC) scheme [1], [3]. For ALOHA type of MAC, the interference can still be correlated in time when there are correlations in the fading channel and/or the user mobility.

Keeping in mind the ongoing standardization activities for the deployment of commercial millimeter-wave wireless (mmW) networks, and the deployment of urban street micro-cells also in non-mmW frequencies, the impact of blockage and deployment area on the correlation of interference becomes an attractive topic to study. Thus far, the performance analysis of wireless networks usually neglects the correlation of links that share common obstacles [4]–[6]. In [7], the impact of shadowing correlations on the joint coverage probability at different locations is studied. The study in [7] does not discuss the joint impact of user density and blockage density on the temporal correlation of interference.

In this paper, we consider a continuous and bounded one-dimensional (1D) deployment, and we study the temporal correlation of interference for static users, and users with independent and identically distributed (i.i.d.) locations over time. The former is useful for studying static networks. The latter can be used to calculate the correlation of interference in highly moving networks and/or the long-term interference correlation in networks with asymptotic independent mobility, e.g., random walk, Brownian motion, constrained i.i.d. mobility with wrap around or bouncing back [1], [8], Random Waypoint Mobility (RWPM) [9], etc. Studying interference correlation with uncorrelated mobility will also highlight that a

bounded domain and/or a domain with blockage can make the interference pattern correlated too. Even though the analysis in the 1D space seems to be an over-simplification, it allows getting useful insights about the correlation of interference at a low complexity. The 1D scenario can also find practical applications, e.g., in vehicular networks.

Next, we summarize the most important insights about the system behaviour which, to the best of our knowledge, are new: (i) With uncorrelated user mobility, the temporal correlation of interference becomes inversely proportional to the size of the deployment domain when there is no blockage. (ii) With a finite density of blockage, the correlation coefficient stays positive, even if the deployment area is infinite. (iii) In the static case, blockage increases the correlation of interference. (iv) With uncorrelated mobility, there is a critical user-to-blockage density ratio that determines the correlation of interference as compared to the case without blockage. At a high density of blockage, the critical ratio can be expressed in a closed-form.

## II. SYSTEM MODEL

We consider two independent Poisson Point Processes (PPPs), one for the users and the other for the blockage, over the line segment  $[-V, V]$ ,  $V \geq 1$ . The density of users is  $\lambda$  and the density of blockage is  $\mu$ . We use slotted ALOHA MAC scheme, where every user transmits with probability  $\xi$ , independently of other users and of its own transmissions in previous time slots. We use a bounded distance-based propagation pathloss model,  $l(r) = \min\{1, r^{-a}\}$ , where  $r$  is the distance and  $a \geq 2$  is the pathloss exponent. We model the fast fading by the Rayleigh distribution with unit mean. Also, there is correlated slow fading due to blockage. The locations of obstacles are fixed but unknown. The obstacles do not hinder the user moves but they attenuate the user signal. It is assumed that the penetration loss per obstacle is uniformly distributed on  $[0, \gamma]$ ,  $\gamma \leq 1$ .

Assuming common transmit power level  $P_t$  for all users, the interference at time slot  $t$  and location  $y_p \in [-V, V]$  is

$$\mathcal{I}(t) = P_t \sum_{i=1}^k \xi_i(t) h_i(t) \beta_i(t) l(x_i(t) - y_p)$$

where  $k$  is a particular realization of the PPP governing the distribution of users,  $\xi_i$  is a Bernoulli Random Variable (RV) describing the  $i$ -th user activity,  $\mathbb{E}\{\xi_i\} = \xi \forall i$ ,  $h_i$  is an exponential RV with unit mean modeling Rayleigh fast fading,  $\mathbb{E}\{h_i\} = 1 \forall i$ ,  $\beta_i$  is the RV describing the penetration loss between the  $i$ -th user and the location  $y_p$ , and  $x_i \in [-V, V]$  is a uniform RV modeling the location for the  $i$ -th user.

K. Koufos and C.P. Dettmann are with the School of Mathematics, University of Bristol, BS8 1TW, Bristol, UK. {K.Koufos, Carl.Dettmann}@bristol.ac.uk

J.P. Coon is with the Department of Engineering Science, University of Oxford, Oxford, OX1 3PJ, UK. justin.coon@eng.ox.ac.uk

This work was supported by the EPSRC grant numbers EP/N002458/1 and EP/N002350/1 for the project Spatially Embedded Networks.

The distribution of  $\beta_i$  is difficult to obtain in terms of simple functions, however the moments of the penetration loss at distance  $d_i = |x_i - y_p|$ , i.e., between the  $i$ -th user and the location  $y_p$  can be computed as  $\mathbb{E}\{\beta_i^s\} = e^{-\mu d_i(1-\frac{1}{1+\gamma^s})}$  [6], [10]. Even though the users are distributed independently of each other, they may be blocked by some common obstacles. The first-order cross-moment of penetration loss for two users  $i, j$  depends on the relative locations of  $x_i, x_j$  w.r.t.  $y_p$ . When the two links  $x_i \rightarrow y_p$  and  $x_j \rightarrow y_p$  do not share any obstacles, the penetration losses are uncorrelated,  $\mathbb{E}\{\beta_i \beta_j\} = e^{-\mu(d_i+d_j)(1-\frac{1}{2})}$ . Otherwise,  $\mathbb{E}\{\beta_i \beta_j\} = e^{-\mu \min\{d_i, d_j\}(1-\frac{1}{3}\gamma^2)} e^{-\mu |d_i - d_j|(1-\frac{1}{2}\gamma)}$  [10].

In what follows, we will make use of the Moment Generating Function (MGF) to analyze the moments of interference. The MGF of interference at time slots  $t, \tau$  is

$$\Phi_{\mathcal{I}} = \iiint \sum_{\xi, k} e^{s_1 \mathcal{I}(t) + s_2 \mathcal{I}(\tau)} f_{\xi, \beta} f_{\xi} f_h \text{Po}(\lambda) dx dh d\beta$$

where  $\xi, h, x$  and  $\beta$  are vectors of RVs with elements,  $\xi_i, h_i, x_i$  and  $\beta_i \forall i$  at time slots  $t, \tau$ ,  $\text{Po}(\lambda) = \frac{e^{-2\lambda V} (2\lambda V)^k}{k!}$  stands for the Poisson distribution of the number of users with realization  $k$ , and the arguments in the Probability Distribution Functions are omitted for brevity.

In order to assess the correlation of interference at time slots  $t, \tau$  we use the Pearson correlation coefficient, i.e., the ratio of the covariance of RVs  $\mathcal{I}(t), \mathcal{I}(\tau)$  divided by the product of their standard deviations. We consider static users with fixed but unknown locations, and users with i.i.d. locations over time, i.e., a new realization of users is drawn in every time slot. In both cases, the statistics of interference are independent of the time slots  $t, \tau$  we take the measurements and the time-lag  $|t - \tau|$ . Therefore the Pearson correlation coefficient becomes

$$\rho = \frac{\mathbb{E}\{\mathcal{I}(t)\mathcal{I}(\tau)\} - \mathbb{E}\{\mathcal{I}(t)\}^2}{\mathbb{E}\{\mathcal{I}^2(t)\} - \mathbb{E}\{\mathcal{I}(t)\}^2}. \quad (1)$$

For the static case, we denote the correlation coefficient by  $\rho_0$ . For the mobile case, we denote it by  $\rho_\infty$ . The correlation coefficient is location-dependent but we omit the related index for brevity. We will show how to calculate the coefficients  $\rho_0, \rho_\infty$  at the origin. The expressions at an arbitrary point  $y_p \in [-V, V]$  can be obtained in a similar manner.

### III. INTERFERENCE MEAN AND VARIANCE

The mean of interference is computed after evaluating the first derivative of the MGF  $\frac{\partial \Phi_{\mathcal{I}}}{\partial s_1}$  at  $s_1 = 0$ .

$$\begin{aligned} \mathbb{E}\{\mathcal{I}\} &\stackrel{(a)}{=} \sum_k k \mathbb{E}\{h_i\} \mathbb{E}\{\xi_i\} \iint \beta_i l(x_i) f_{\beta_i, x_i} d\beta_i dx_i \text{Po}(\lambda) \\ &\stackrel{(b)}{=} 2\lambda \xi \left( \frac{2(1 - e^{-\frac{\mu(2-\gamma)}{2}})}{\mu(2-\gamma)} + E_a\left(\frac{\mu(2-\gamma)}{2}\right) - \frac{E_a(\frac{\mu(2-\gamma)V}{2})}{V^{a-1}} \right) \end{aligned} \quad (2)$$

where (a) follows from the fact that the users are indistinct and  $i$  is a typical user, (b) uses that the penetration loss  $\beta_i$  depends on the location  $x_i$  and also averages over the Poisson distribution  $\text{Po}(\lambda)$ ,  $E_n(z) = \int_1^\infty t^{-n} e^{-zt} dt$  is the generalized exponential integral, and the transmit power level has been taken equal to  $P_t = 1$ .

The second moment of interference is

$$\begin{aligned} \mathbb{E}\{\mathcal{I}^2\} &= 2\lambda \xi \int_{-V}^V \mathbb{E}\{\beta_x^2\} l^2(x) dx + \sigma \\ &= 4\lambda \xi \left( \frac{3}{\mu(3-\gamma^2)} \left( 1 - e^{-\frac{1}{3}\mu(3-\gamma^2)} \right) + E_{2a}\left(\frac{\mu}{3}(3-\gamma^2)\right) - \right. \\ &\quad \left. \frac{1}{V^{2a-1}} E_{2a}\left(\frac{1}{3}\mu(3-\gamma^2)V\right) \right) + \sigma \end{aligned} \quad (3)$$

where it has been used that  $\mathbb{E}\{h^2\} = 2, \mathbb{E}\{\xi^2\} = \xi$ , and the term  $\sigma$  captures the correlation in the interference levels generated by different users

$$\sigma = \lambda^2 \xi^2 \int_{-V}^V \int_{-V}^V \mathbb{E}\{\beta_x \beta_y\} l(x) l(y) dy dx. \quad (4)$$

The calculation of  $\sigma$  can be split into two terms,  $\sigma = \sigma_1 + \sigma_2$ , depending on whether pairs of links share common obstacles or not. The uncorrelated part is equal to  $\sigma_1 = \frac{1}{2} \mathbb{E}\{\mathcal{I}\}^2$ , and the correlated part can be written as  $\sigma_2 = 4\lambda^2 \xi^2 \int_0^V \int_0^x \mathbb{E}\{\beta_x \beta_y\} l(x) l(y) dy dx$ . In order to calculate  $\sigma_2$ , one has to take care of the piecewise nature of the pathloss model. For a positive  $\gamma$ , we finally get

$$\begin{aligned} \sigma_2 &= 4\lambda^2 \xi^2 \left( 6 \frac{3(2-\gamma)e^{-\frac{1}{3}\mu(3-\gamma^2)} + \gamma(3-2\gamma) - 2(3-\gamma^2)e^{-\frac{1}{2}\mu(2-\gamma)}}{\mu\gamma^2(2-\gamma)(3-2\gamma)(3-\gamma^2)} + \right. \\ &\quad \left. \frac{6(2-\gamma)(1 - e^{-\frac{1}{6}\mu\gamma(3-2\gamma)}) (E_a(\frac{\mu(2-\gamma)}{2}) - E_a(\frac{\mu(2-\gamma)V}{2}))}{\mu\gamma(6-7\gamma+2\gamma^2)} + \right. \\ &\quad \left. E_a\left(\frac{\mu\gamma(3-2\gamma)}{6}\right) \left( E_a\left(\frac{\mu(2-\gamma)}{2}\right) - V^{1-a} E_a\left(\frac{\mu(2-\gamma)V}{2}\right) \right) + \right. \\ &\quad \left. \int_1^V e^{-\frac{1}{2}\mu(2-\gamma)x} x^{1-2a} E_a\left(\frac{1}{6}\mu\gamma(3-2\gamma)x\right) dx \right). \end{aligned} \quad (5)$$

In equation (5), the integral  $I_0 = \int_1^V e^{-cx} x^{1-2a} E_a(bx) dx$ , where  $c = \frac{\mu(2-\gamma)}{2}$  and  $b = \frac{\mu\gamma(3-2\gamma)}{6}$  has the least contribution of the four terms. It can be computed in terms of the incomplete Gamma function only if the constants  $c, b$  are equal. This is not true unless  $\mu = 0$ , where the integral becomes trivial to solve and equals to  $\frac{1-V^{2(1-a)}}{2(a-1)^2}$ . For a positive  $\mu$ , the integral decays sharply with  $x$ . One may avoid numerical integration, and use the Laplace method to approximate it instead. Due to the lack of space, we give only the second-order approximation for  $V \rightarrow \infty$ ,  $I_0 \approx e^{-c+\log E_a(b)} \left( \frac{1}{A} - \frac{2B}{A^3} \right)$ , where  $A = 2a-1+c - \frac{bE_{a-1}(b)}{E_a(b)}$ ,  $B = \frac{b^2 E_{a-2}(b)}{2E_a(b)} - \frac{b^3 E_{a-1}(b)^2}{2E_a(b)^2} - \frac{2a-1}{2}$ . Even this has sufficient accuracy for our problem.

For impenetrable blockage, one has to substitute  $\gamma = 0$  in equations (2), (3). For  $\gamma = 0$ , equation (5) becomes indefinite. One should use  $\sigma_2 = 4\lambda^2 \xi^2 \left( \frac{1-(1+\mu)e^{-\mu}}{\mu^2} + \frac{a}{a-1} \left( E_a(\mu) - \frac{E_a(\mu V)}{V^{a-1}} \right) + \frac{V^{2(1-a)} E_{2a-1}(\mu V) - E_{2a-1}(\mu)}{a-1} \right)$  instead.

### IV. TEMPORAL INTERFERENCE CORRELATION

The cross-correlation of interference can be computed from the first-order cross-derivative of the MGF,  $\frac{\partial^2 \Phi_{\mathcal{I}}}{\partial s_1 \partial s_2}$  at  $(s_1, s_2) = (0, 0)$ . For the static case, the penetration losses of a single user at different time slots are fully correlated. Hence,

$$\mathbb{E}\{\mathcal{I}(t)\mathcal{I}(\tau)\} = \lambda \xi^2 \mathcal{I} + \sigma \quad (6)$$

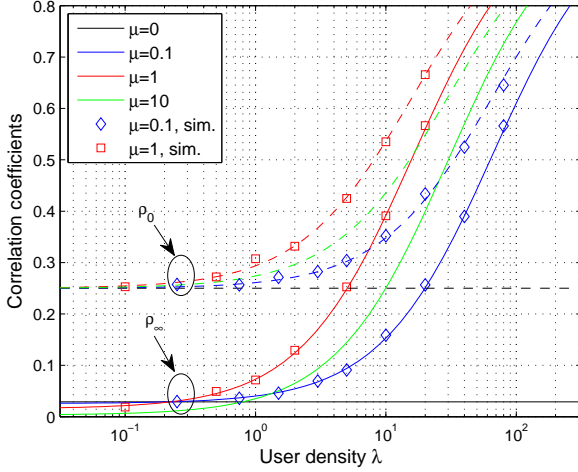


Fig. 1. Correlation coefficients of interference  $\rho_0, \rho_\infty$  w.r.t. the user density. Minimum penetration loss  $\gamma = 1$ , pathloss exponent  $\alpha = 2$ , size of the deployment domain  $V = 25$  and user activity  $\xi = 0.5$ . For  $\mu = 0.1$  and  $\mu = 1$  the models are validated with simulations.

where  $I = \int_{-V}^V \mathbb{E}\{\beta_x^2\} l^2(x) dx$  is computed as in (3).

With uncorrelated user locations over time, the penetration losses may still be correlated. Hence,

$$\mathbb{E}\{\mathcal{I}(t)\mathcal{I}(\tau)\} = \frac{\lambda \xi^2}{2V} \int_{-V}^V \int_{-V}^V \mathbb{E}\{\beta_x \beta_y\} l(x) l(y) dx dy + \sigma. \quad (7)$$

Using equation (4), the first term in equation (7) can also be written as  $\frac{\sigma}{2\lambda V}$ . The correlation coefficients are computed after substituting equations (6), (7) in equation (1)

$$\rho_0 = \frac{\lambda \xi^2 I + \sigma - \mathbb{E}\{\mathcal{I}\}^2}{2\lambda \xi I + \sigma - \mathbb{E}\{\mathcal{I}\}^2}, \quad \rho_\infty = \frac{\frac{\sigma}{2\lambda V} + \sigma - \mathbb{E}\{\mathcal{I}\}^2}{2\lambda \xi I + \sigma - \mathbb{E}\{\mathcal{I}\}^2}. \quad (8)$$

**Lemma 1.** Without blockage, both coefficients  $\rho_0, \rho_\infty$  are positive provided that the area  $V$  is finite.

*Proof.* Without blockage,  $\mu = 0$ , the interference levels generated by different users become uncorrelated, i.e.,  $\sigma = \mathbb{E}\{\mathcal{I}\}^2$ . After substituting  $\sigma = \mathbb{E}\{\mathcal{I}\}^2$  in equation (8), and this back in (1), we get  $\rho_0|_{\mu=0} = \frac{\xi}{2} > 0$ , and

$$\rho_\infty|_{\mu=0} = \frac{\mathbb{E}\{\mathcal{I}\}^2}{4\lambda^2 \xi V I} = \frac{\xi (a - V^{1-a})^2 (2a - 1)}{2V(a - 1)^2 (2a - V^{1-2a})} > 0. \quad (9)$$

□

**Lemma 2.** For infinite area  $V$ ,  $\rho_\infty|_{\mu=0} = 0$  and  $\rho_\infty > 0$ .

*Proof.* From equation (9),  $\lim_{V \rightarrow \infty} \rho_\infty|_{\mu=0} = 0$ . Also,  $\lim_{V \rightarrow \infty} \frac{\sigma}{2\lambda V} = 0$ . Hence, from equation (8),  $\lim_{V \rightarrow \infty} \rho_\infty = \lim_{V \rightarrow \infty} \frac{\sigma - \mathbb{E}\{\mathcal{I}\}^2}{2\lambda \xi I + \sigma - \mathbb{E}\{\mathcal{I}\}^2} > 0$  for  $\mu > 0$ . □

**Lemma 3.** There is a user density  $\lambda^*$  where  $\rho_\infty^* = \rho_\infty|_{\mu=0}$ .

*Proof.* Using that the Pearson correlation coefficient is at most equal to one, one can show that the first derivative of  $\rho_\infty$  in equation (8) w.r.t.  $\lambda$  is positive. Also,  $\lim_{\lambda \rightarrow \infty} \rho_\infty = 1 > \frac{\xi}{2} =$

$$\rho_0|_{\mu=0} > \rho_\infty|_{\mu=0}, \text{ and } \lim_{\lambda \rightarrow 0} \rho_\infty = \frac{\xi \int_{-V}^V \int_{-V}^V \mathbb{E}\{\beta_x \beta_y\} l(x) l(y) dy dx}{4V \int_{-V}^V \mathbb{E}\{\beta_x^2\} l^2(x) dx} \leq$$

$\frac{\xi \int_{-V}^V \int_{-V}^V l(x) l(y) dy dx}{4V \int_{-V}^V l^2(x) dx} = \rho_\infty|_{\mu=0}$  due to the Cauchy inequality.

Therefore with uncorrelated mobility, blockage reduces the correlation of interference at low user densities, while the opposite is true at high user densities, and the existence of user density  $\lambda^*$  is proved. □

**Lemma 4.** At a high density of blockage, the correlation coefficients increase with the user-to-blockage density ratio.

*Proof.* Let us denote by  $p = \frac{\lambda}{\mu}$  the user-to-blockage density ratio. If we expand the moments around  $\mu \rightarrow \infty$ , we get  $\mathbb{E}\{\mathcal{I}\} \approx \frac{2p\xi}{2-\gamma}$ ,  $\sigma_2 \approx \frac{24p^2\xi^2}{(2-\gamma)(3-\gamma^2)}$ ,  $\mathbb{E}\{\mathcal{I}^2\} \approx \frac{12p\xi}{3-\gamma^2} + \sigma$ . After substituting these approximations in equation (8), the coefficients  $\rho_0$  and  $\rho_\infty$  around  $\mu \rightarrow \infty$ , keeping  $p$  finite or  $p \rightarrow 0$ , can be read as

$$\begin{aligned} \rho_0|_{\mu \rightarrow \infty} &= \frac{3\xi(2-\gamma)^2 + 12\xi p(2-\gamma) - 4\xi p(3-\gamma^2)}{6(2-\gamma)^2 + 12\xi p(2-\gamma) - 4\xi p(3-\gamma^2)} = \frac{\xi}{2} + \\ &\quad \frac{(3-3\gamma+\gamma^2)(2-\xi)p}{3(2-\gamma)^2} - \frac{2(3-3\gamma+\gamma^2)^2(2-\xi)\xi^2 p^2}{9(2-\gamma)^4} + \mathcal{O}(p)^3 \\ \rho_\infty|_{\mu \rightarrow \infty} &= \frac{(1 + \frac{1}{2\lambda V})6\xi p(2-\gamma) - (\frac{1}{2} - \frac{1}{2\lambda V})4\xi p(3-\gamma^2)}{3(2-\gamma)^2 + 6\xi p(2-\gamma) - 2\xi p(3-\gamma^2)} = \frac{3\xi p}{2-\gamma} - \\ &\quad \frac{2\xi(3-\gamma^2)p}{3(2-\gamma)^2} - \frac{(6\xi(2-\gamma) - 2\xi(3-\gamma^2))^2 p^2}{9(2-\gamma)^4} + \mathcal{O}(p)^3 \end{aligned} \quad (10)$$

where in the expression of  $\rho_\infty|_{\mu \rightarrow \infty}$ , the contribution of the terms  $\frac{1}{2\lambda V}$  has been omitted from the series expansion. This approximation is valid for  $2\lambda V \gg 1$ .  $\rho_\infty|_{\mu \rightarrow \infty}$  is increasing in  $p$  for  $\gamma \leq 1$ , and  $\rho_0|_{\mu \rightarrow \infty}$  is increasing in  $p$  for  $\xi \leq 1$ . □

In Fig. 1, we have used equation (8) to compute the correlation coefficients  $\rho_0, \rho_\infty$  for various user and blockage densities. In the static case, blockage makes the propagation pathloss of different users correlated resulting in higher correlation coefficients than in the case without blockage. In the mobile case, the impact of blockage on the interference correlation depends on the user density, see Lemma 3. When the user density is low, the interference level is also low, on average, and it would vary significantly with mobility because of the transitions in the propagation conditions, from Line-of-Sight (LoS) to Non-Line-of-Sight (NLoS) and vice versa.<sup>1</sup> These transitions make the correlation of interference less than in the case without blockage. On the other hand, when the user density is high, the correlation of penetration losses among the user prevails, and mobility does not help much in reducing it. Some users will transit from LoS to NLoS but at the same time, some others with transit from NLoS to LoS. Overall, the interference level will not vary significantly. When  $\mu = 10$ , the approximations for a high density of blockage in equation (10) become valid. For the parameter settings used to generate Fig. 1,  $\gamma = 1, \xi = 1$ , we get  $\rho_\infty|_{\mu \rightarrow \infty} \approx \frac{2p}{3+2p}$  after neglecting the contribution of the term  $\frac{1}{2\lambda V}$ . From equation (9), after neglecting the contribution of the terms  $V^{1-a}, V^{1-2a}$ , we get  $\rho_\infty|_{\mu=0} \approx \frac{3}{2V}$  for  $a = 2$ . Therefore,  $\rho_\infty|_{\mu \rightarrow \infty} \geq \rho_\infty|_{\mu=0}$  for  $\lambda \geq \lambda^*, \lambda^* = \frac{9\mu}{4V-6} \approx 0.95$ , see Fig. 1. To sum up, for a high density of blockage, the critical user-to-blockage density ratio can be expressed in terms of the size of the deployment area  $V$ , the channel model  $a, \gamma$  and the user activity  $\xi$ .

<sup>1</sup>By LoS propagation conditions it is meant that the link between the user and the origin is free from obstacles while multipath fading is still present.

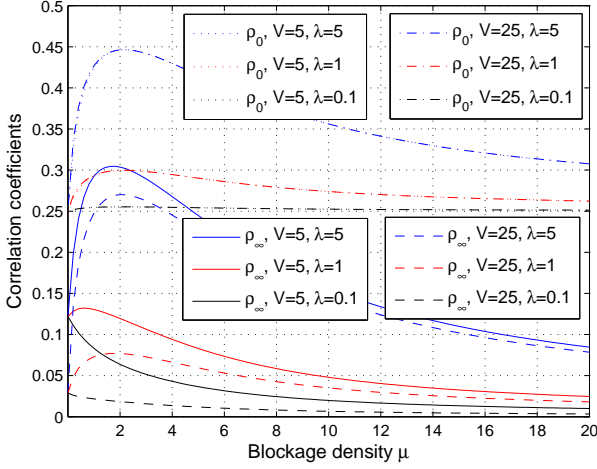


Fig. 2. Correlation coefficients of interference  $\rho_0, \rho_\infty$  w.r.t. the blockage density. The parameter settings are available in the caption of Fig. 1, unless otherwise stated in the legend.

When the user density is fixed and finite and the blockage density keeps on increasing, the correlation of penetration losses from different users starts to reduce beyond a certain density of blockage. As a result, the correlation coefficients  $\rho_0, \rho_\infty$  will reduce too, see Fig. 2 and Lemma 4. In Fig. 2, we also see that smaller domains  $V$  are associated with higher correlation coefficients  $\rho_\infty$ . This is because a smaller domain results in less randomness in the distance-based propagation pathloss of a user at different time slots. Obviously, the impact of distance-based pathloss on the interference is more prominent at low blockage densities. In the static case, the size of the deployment domain does not impact much the correlation of interference. The curves for different domains  $V$  in Fig. 2 practically overlap.

To get a glimpse on the location-dependent properties of interference correlation, we also study it at the boundary,  $y_p = V$ . Without blockage, the correlations coefficients are  $\rho_0|_{\mu=0} = \frac{\xi}{2}$  and  $\rho_\infty|_{\mu=0} \approx \frac{\xi(a-V^{1-a})^2(2a-1)}{4V(a-1)^2(2a-V^{1-2a})}$ . After comparing it with equation (9), we see that the correlation coefficient  $\rho_\infty|_{\mu=0}$  at the boundary is half the coefficient  $\rho_\infty|_{\mu=0}$  at the center. This is due to the fact that at the boundary there is more randomness in the distance-based pathloss as compared to the center.

With blockage, the coefficient  $\rho_0$  at the boundary will be marginally higher than the coefficient  $\rho_0$  at the center, because the boundary sees more correlated penetration losses. On the other hand, the coefficient  $\rho_\infty$  is smaller at the boundary than at the center, see Fig. 3. This is because at the boundary, where the level of interference is also less, the randomness in the link gain is higher. For increasing density of blockage, the generated interference is dominated from the users located close to the boundary. Therefore the higher randomness of the link gain starts to vanish and the correlation becomes less sensitive to the location, see Fig. 3. It can be shown that for a high density of blockage, the coefficient  $\rho_\infty$  at the boundary can also be approximated by the expression in equation (10).

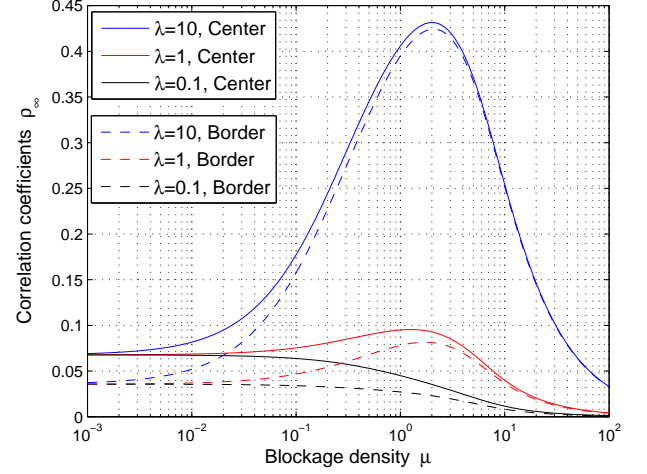


Fig. 3. Correlation coefficients  $\rho_\infty$  at the origin and at the boundary w.r.t. the blockage density. The size of the domain is  $V=10$ . The rest of parameter settings are available in the caption of Fig. 1.

## V. CONCLUSIONS

In this letter, we showed that a bounded domain and/or a domain with blockage can induce temporal correlation of interference even if the user locations are uncorrelated over time. With blockage, the correlation coefficient increases with the density of users. Therefore beamforming techniques, which essentially scale down the density of users generating interference, will scale down the temporal correlation of interference too. Extending the results of this paper in two-dimensional areas with beamforming and nonuniform distribution of users, e.g., due to RWPM mobility is a topic for future work.

## REFERENCES

- [1] Z. Gong and M. Haenggi, "Interference and Outage in Mobile Random Networks: Expectation Distribution and Correlation", *IEEE Trans. Mobile Comput.*, vol. 13, pp. 337-349, Feb. 2014.
- [2] S. Krishnan and H.S.Dhillon, "Spatio-temporal Interference Correlation and Joint Coverage in Cellular Networks", available at <http://arxiv.org/pdf/1606.05332.pdf>
- [3] U. Schilcher, C. Bettstetter and G. Brandner, "Temporal Correlation of Interference in Wireless Networks with Rayleigh Block Fading", *IEEE Trans. Mobile Comput.*, vol. 11, pp. 2109-2120, Dec. 2012.
- [4] T. Bai and R.W. Heath, "Coverage and Rate Analysis for Millimeter-Wave Cellular Networks", *IEEE Trans. Wireless Commun.*, vol. 14, pp. 1100-1114, 2015.
- [5] A. Thornburg, T. Bai and R.W. Heath, "Performance Analysis of mmWave Ad Hoc Networks", available at <http://arxiv.org/abs/1412.0765>.
- [6] T. Bai, R. Vaze and R.W. Heath, "Analysis of Blockage Effects on Urban Cellular Networks", *IEEE Trans. Wireless Commun.*, vol. 13, pp. 5070-5083, 2014.
- [7] F. Baccelli and X. Zhang, "A Correlated Shadowing Model for Urban Wireless Networks", *IEEE Int. Conf. Comput. Commun. (INFOCOM)*, Apr. 2015, pp. 801-809.
- [8] C. Bettstetter, "Mobility Modeling in Wireless Networks: Categorization, Smooth Movement, and Border Effects", *ACM Mobile Comput. and Commun. Review*, 2001.
- [9] C. Bettstetter, G. Resta and P. Santi, "The Node Distribution of the Random Waypoint Mobility Model for Wireless Ad Hoc Networks", *IEEE Trans. Mobile Comput.*, vol. 2, pp. 257-269, Jul.-Sept. 2003.
- [10] K. Koufos and C.P. Dettmann, "Temporal Correlation of Interference in Bounded Mobile Ad Hoc Networks with Blockage", available at <https://arxiv.org/pdf/1606.01840v2.pdf>.